More light on Higgs flavor at the LHC: Higgs boson couplings to light quarks through $h+\gamma$ production

J. A. Aguilar-Saavedra,[1,2,*] J. M. Cano,[2,3,†] and J. M. No[2,3,‡]

[1]*Departamento de Física Teórica y del Cosmos, Universidad de Granada, E-18071 Granada, Spain*
[2]*Instituto de Física Teórica, IFT-UAM/CSIC, Cantoblanco, 28049 Madrid, Spain*
[3]*Departamento de Física Teórica, Universidad Autonoma de Madrid, Cantoblanco, 28049 Madrid, Spain*

(Received 9 September 2020; revised 4 February 2021; accepted 27 April 2021; published 24 May 2021)

Higgs production in association with a photon at hadron colliders is a rare process, not yet observed at the LHC. We show that this process is sensitive to significant deviations of Higgs couplings to first- and second-generation SM quarks (particularly the up type) from their SM values, and we use a multivariate neural network analysis to derive the prospects of the High Luminosity LHC to probe deviations in the up and charm Higgs Yukawa couplings through $h+\gamma$ production.

DOI: 10.1103/PhysRevD.103.095023

I. INTRODUCTION

Whereas the Yukawa couplings of the 125 GeV Higgs boson to third-generation Standard Model (SM) fermions have been measured rather precisely at the Large Hadron Collider (LHC), the values of the corresponding Higgs boson couplings to light SM fermions are still weakly (or very weakly, for first-generation fermions) constrained. In the last few years, there has been an important theoretical [1–15] and experimental [16–22] effort to probe the charm-quark Yukawa coupling, as well as the rest of the light SM quarks (see, e.g., Refs. [2,3,8]). Some of the proposed methods to probe the Yukawa couplings of the light SM quarks at the LHC are quark-flavor specific (they rely on tagging/identifying a specific flavor in the final state—e.g., a charm-quark jet produced in association with a Higgs boson [7], or a strange-flavored meson from a rare Higgs decay process [2]), yet others could be sensitive to deviations in any of the Higgs couplings to first- and second-generation SM quarks. Altogether, there exists a strong interplay among all these different probes, which are key to unraveling the details of the mass-generation mechanism for the first two generations of matter: while the LHC will not be sensitive enough to probe the SM values of the corresponding Higgs Yukawa couplings, it will explore beyond-the-SM scenarios with significant enhancements in these Yukawa couplings (see Refs. [23–29] for some examples).[1] Our current lack of understanding of the pattern of Higgs Yukawa couplings motivates probing such enhancements to gain insight on the entire Higgs flavor structure, as well as to provide the strongest possible experimental constraints on these couplings (even if they are still far from the SM-predicted values).

In this paper, we explore a complementary probe of the Higgs couplings to light SM quarks through the production of a Higgs boson in association with a photon at hadron colliders, $pp \to h\gamma$ (see Refs. [31–37] for other Higgs + photon LHC studies). This is a rare process in the SM, with the leading-order (LO) gluon-initiated contribution $gg \to h\gamma$ [see Fig. 1 (left)] vanishing due to Furry's theorem [38,39]. The largest contributions to the inclusive $h\gamma$ production at the LHC include extra objects with high transverse momentum in the final state [34]. In the absence of such extra final-state particles besides the Higgs boson and photon, the contribution to Higgs + photon production at the LHC from bottom-antibottom ($b\bar{b}$) and charm-anticharm ($c\bar{c}$) initial states [see Fig. 1 (right)] becomes important, making this process sensitive to the respective Higgs Yukawa couplings y_b and y_c. In addition, the presence of a large deviation from its SM value in the Yukawa couplings of the quarks $q = s, u, d$ (strange, up, and down) would greatly enhance the corresponding $q\bar{q}$-initiated contribution from Fig. 1 (right). These contributions are at the same time proportional to the square of the quark electric charge Q_q, which suppresses the cross section for down-type quark-initiated $q\bar{q} \to h\gamma$ processes relative to up-type quark-initiated processes by a factor $(Q_u/Q_d)^2 = 4$. We thereby study the sensitivity of this

*jaas@ugr.es
†josem.cano@uam.es
‡josemiguel.no@uam.es

[1]Large enhancements of Higgs Yukawa couplings to light quarks can also impact other physical observables—see, e.g., Ref. [30].

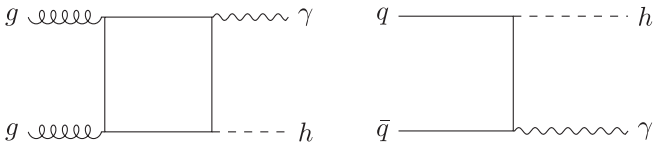

FIG. 1. Left: Feynman diagram for $gg \to h\gamma$, whose amplitude vanishes due to Furry's theorem. Right: example tree-level Feynman diagram for $q\bar{q} \to h\gamma$ (with $q = u, d, s, c, b$) in the SM.

process to the value of the Yukawa coupling y_q for $q = u, c$ at the High Luminosity (HL) LHC, focusing on (in our view) the most promising Higgs decay channel for this purpose, $h \to WW^* \to \ell\nu\ell\nu$ (with ℓ being electrons/muons).

II. $h+\gamma$ PRODUCTION AT THE LHC

As outlined in the Introduction, the dominant $q\bar{q}$-initiated contributions to the exclusive production of a 125 GeV Higgs boson in association with a photon at hadron colliders [see Fig. 1 (right)] are proportional to the square of the corresponding light quark Yukawa coupling y_q^2, evaluated at the scale of the Higgs mass m_h. The running masses for the bottom, charm, and up quarks, evaluated at the scale $m_h = 125$ GeV, are given in the tadpole-free pure $\overline{\text{MS}}$ scheme by $m_b(m_h) = 2.777$ GeV, $m_c(m_h) = 0.605$ GeV, and $m_u(m_h) = 0.0013$ GeV [40], with the SM values of the Yukawa couplings at this scale given by $y_q^{\text{SM}}(m_h) = \sqrt{2}m_q(m_h)/v$, and v being the electroweak (EW) scale. We then parametrize the departure of the Higgs Yukawa couplings to light quarks from their SM values as $\kappa_q = y_q(m_h)/y_q^{\text{SM}}(m_h)$.

The respective $\sqrt{s} = 14$ TeV center-of-mass (c.m.) LHC cross sections at LO for $b\bar{b} \to h\gamma$, $c\bar{c} \to h\gamma$, and $u\bar{u} \to h\gamma$ evaluated with MadGraph 5 [41], for a photon with transverse momentum $p_T^\gamma > 20$ GeV and pseudorapidity $|\eta^\gamma| < 2.5$, using the NNPDF31_NNLO_AS_0118_LUXQED [42] parton distribution function (PDF) set, are

$$\sigma_{b\bar{b}} = \kappa_b^2 \times 0.397 \text{ fb}, \qquad \sigma_{c\bar{c}} = \kappa_c^2 \times 0.160 \text{ fb},$$
$$\sigma_{u\bar{u}} = \kappa_u^2 \times 5.16 \times 10^{-3} \text{ ab}. \tag{1}$$

For the SM, the $c\bar{c}$ contribution is found to be smaller but comparable to $\sigma_{b\bar{b}}$ (despite the large hierarchy between Yukawa couplings), owing to the relative $(Q_c/Q_b)^2 = 4$ factor and larger PDF of the charm quark with respect to the bottom quark. At the same time, while $\sigma_{u\bar{u}}$ in the SM is negligible, an enhancement of the up-quark Yukawa making it comparable to the SM charm Yukawa $y_u(m_h) \sim y_c^{\text{SM}}(m_h)$ (corresponding to $\kappa_u \sim 500$) would raise the $u\bar{u}$-initiated $h\gamma$ cross section to ~1.3 fb.[2] This might allow for a test of first- vs second-generation Yukawa universality in the up-quark sector at the HL-LHC with 3 ab^{-1} of integrated luminosity via this process. We also note that subdominant contributions to the $q\bar{q} \to h\gamma$ exclusive production, such as $q\bar{q} \to \gamma^*/Z^* \to h\gamma$, quickly become negligible for sizable light Yukawa enhancements—e.g., for $\kappa_c \sim 3$, their size is ~5% of the $\sigma_{b\bar{b}} + \sigma_{c\bar{c}}$ cross section sum.

Before presenting our analysis in the next section, let us discuss briefly the production of a Higgs boson and a photon at the LHC in an inclusive manner, allowing for extra high-p_T objects to be produced in the process. The dominant contributions to the inclusive $h + \gamma$ production are [34,35] vector boson fusion (VBF, $h\gamma jj$) and associated production with a W or Z boson (AP, $h\gamma V$). Slightly smaller than the latter but also important are the production together with a high-p_T jet ($h\gamma j$) and production in association with a top-quark pair ($t\bar{t}h\gamma$). Cross sections for these processes are in the $\mathcal{O}(1\text{–}10)$ fb ballpark, and they do not depend on κ_q (except for small contributions to $h\gamma j$ and $h\gamma jj$, only important for large κ_c values). Thus, to gain sensitivity to the Higgs Yukawa couplings to light quarks, these processes need to be efficiently suppressed in favor of the $b\bar{b}$- and $c\bar{c}$-initiated ones. Fortunately, this may be easily achieved by vetoing extra hard activity in the $h\gamma$ event selection and exploiting the different kinematics of the Higgs boson and photon among these processes, as we will discuss below.

III. SENSITIVITY VIA $h \to WW^* \to \ell\nu\ell\nu$

In the remainder of this work, we focus on the $h \to WW^* \to \ell^+\nu\ell^-\bar{\nu}$ decay of the Higgs boson as the most sensitive channel for our purposes. Other Higgs decay choices like $h \to b\bar{b}$ and $h \to \tau^+\tau^-$ face very large SM backgrounds, or suffer from very small decay branching fractions, as is the case of $h \to \gamma\gamma$ and $h \to ZZ^* \to 4\ell$.

To search for the $h\gamma$ signature via the decay $h \to WW^* \to \ell^+\nu\ell^-\bar{\nu}$ at the LHC with $\sqrt{s} = 14$ TeV c.m. energy, we select events with exactly two oppositely charged leptons (electrons or muons) and a photon with pseudorapidities $|\eta^{\ell,\gamma}| < 4$. The transverse momentum of the photon is required to satisfy $p_T^\gamma > 25$ GeV, and the transverse momenta of the leading (ℓ_1) and subleading (ℓ_2) leptons need to satisfy $p_T^{\ell_1} > 18$ GeV, $p_T^{\ell_2} > 15$ GeV or $p_T^{\ell_1} > 23$ GeV, $p_T^{\ell_2} > 9$ GeV, following Run 2 ATLAS dilepton triggers [43]. Dilepton trigger thresholds are in fact expected to lower for HL-LHC [44], and a dilepton + photon trigger with lower thresholds could also be implemented. We also require the missing transverse energy in the event to be $\not{E}_T > 35$ GeV. In order to suppress events with extra high-p_T activity, we veto events having a jet with $p_T > 50$ GeV or having two jets with $p_T > 20$ GeV and a pseudorapidity gap $\Delta\eta^{j_1 j_2} > 3$.

The dominant SM backgrounds are the irreducible processes $pp \to \ell^+\nu\ell^-\bar{\nu}\gamma$ and $pp \to Z\gamma$, $Z \to \tau^+\tau^-$ with

[2]This is a factor ~10 larger than the SM value for $\sigma_{c\bar{c}}$ from Eq. (1) due to the much larger PDF for the up quark inside the proton.

both τ leptons decaying leptonically, together with the reducible background $pp \to t\bar{t}\gamma$ (with $t \to b\ell^+\nu$, $\bar{t} \to \bar{b}\ell^-\bar{\nu}$). The latter can be further suppressed by imposing a b-tagged jet veto on the selected events. We note that the $Z+$ jets and $Z(\to\ell\ell)\gamma$ SM backgrounds have a very large cross section (see, e.g., Refs. [45–47]). However, the above selection—in particular, the $\not{E}_T$ cut—combined with a Z-mass window veto on the invariant mass of the two leptons $|m_Z - m_{\ell\ell}| > 30$ GeV greatly suppresses these processes. Selecting the two leptons in the event to be of opposite flavor (OF) would provide an additional suppression for these backgrounds. In any case, we retain both OF and SF (same-flavor) lepton events,[3] and we disregard $Z+$ jets and $Z(\to\ell\ell)\gamma$ backgrounds altogether.

We generate our signal and SM background event samples (both at LO) in MadGraph 5 [41] with subsequent parton showering and hadronization with PYTHIA 8 [48] and detector simulation via DELPHES v3.4.2 [49], using the anti-k_T algorithm [50] with $R = 0.4$ for jet reconstruction with FastJet [51] and the DELPHES detector card designed for HL-LHC studies. We do not include pileup in our simulation for simplicity: in the experimental measurements, it has been shown that the pileup contamination can be very efficiently removed by using pileup subtraction algorithms such asPUPPI [52], SOFTKILLER [53], or constituent level subtraction [54].

After event selection, the SM background cross sections are 5.08 fb for $pp \to \ell^+\nu\ell^-\bar{\nu}\gamma$, 3.86 fb for $Z\gamma$, $Z \to \tau^+\tau^-$ and 1.07 fb for $t\bar{t}\gamma$, where the latter includes the effect of the various vetoes in the selection. Assuming SM branching fractions for the Higgs boson (we discuss variants of this assumption in the next section), the signal cross section after event selection is 27.6 ab for $\kappa_b = \kappa_u = 1$, $\kappa_c = 10$, and 41.2 ab for $\kappa_b = \kappa_c = 1$, $\kappa_u = 2000$. In the following, we consider independently the possible enhancement of the charm and up-quark Yukawa couplings with respect to their SM values, performing two separate sensitivity studies.

The rich event kinematics allows for an efficient signal discrimination following the initial event selection discussed above. An important role is played by the transverse mass M_T reconstructed out of the dilepton system + missing energy:

$$M_T^2 = \left(\sqrt{M_{\ell\ell}^2 + |\vec{p}_T^{\,\ell\ell}|^2} + \not{E}_T\right)^2 - |\vec{p}_T^{\,\ell\ell} + \vec{\not{E}}_T|^2, \quad (2)$$

with $\vec{p}_T^{\,\ell\ell}$ being the vector sum of the lepton transverse momenta, $M_{\ell\ell}$ the invariant mass of the dilepton system, and $\vec{\not{E}}_T$ the missing transverse momentum of the event. Other key variables are the dilepton invariant mass $M_{\ell\ell}$ itself, the transverse angular separation $\Delta\phi^{(\ell\ell,\not{E}_T)}$ between the dilepton momentum $\vec{p}_T^{\,\ell\ell}$ and missing momentum $\vec{\not{E}}_T$, or the distance $\Delta R \equiv \sqrt{\Delta\phi^2 + \Delta\eta^2}$ between each lepton and the photon $\Delta R^{\ell_1\gamma}$, $\Delta R^{\ell_2\gamma}$. In Fig. 2, we show the M_T (top) and $M_{\ell\ell}$ (middle) distributions for the signal (with $\kappa_b = \kappa_u = 1$, $\kappa_c = 30$) and the dominant SM backgrounds at the HL-LHC. We also show in Fig. 2 (bottom) the normalized $\Delta\phi^{(\ell\ell,\not{E}_T)}$ and $\Delta R^{\ell_2\gamma}$ distributions for the signal and SM backgrounds. Performing a cut-and-count signal selection, $M_T \in [80, 150]$ GeV, $M_{\ell\ell} \in [5, 55]$ GeV, $\Delta R^{\ell_1\gamma} > 1$, $\Delta R^{\ell_2\gamma} > 0.8$, and $\Delta\phi^{(\ell\ell,\not{E}_T)} > 2$ allows us to extract a HL-LHC projected sensitivity $|\kappa_c| < 13.9$ at a

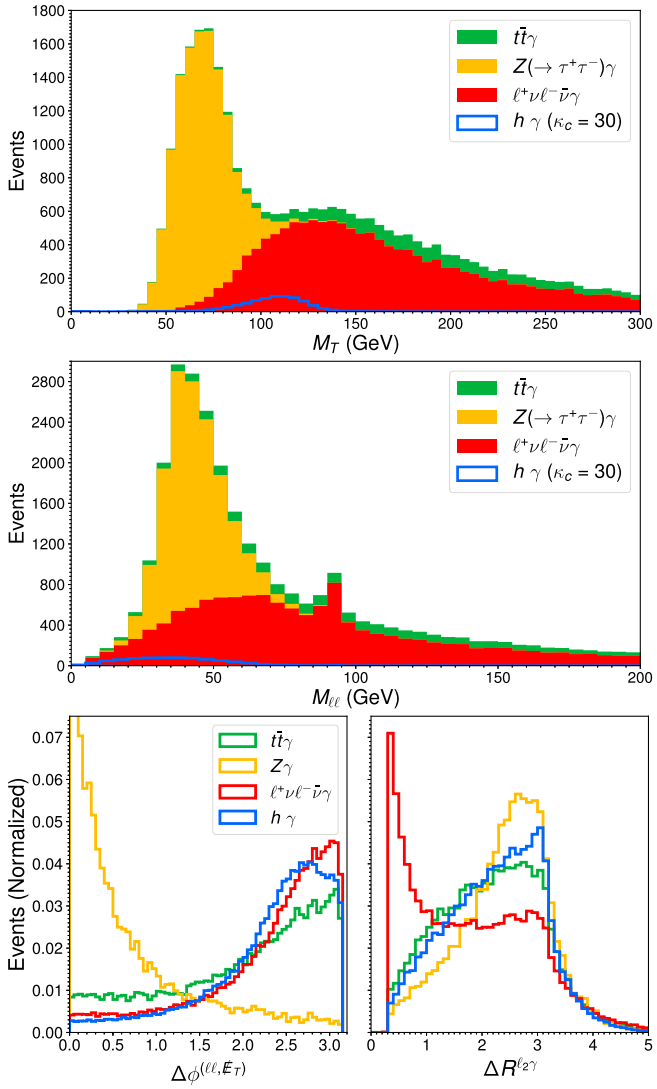

FIG. 2. Top: M_T distribution of events for the dominant SM backgrounds $\ell^+\nu\ell^-\bar{\nu}\gamma$ (red), $t\bar{t}\gamma$ (green), and $Z(\to\tau^+\tau^-)\gamma$ (yellow), all stacked, at the HL-LHC ($\sqrt{s} = 14$ TeV, 3 ab^{-1}). In blue, the corresponding M_T distribution for the $h\gamma$ signal with $\kappa_b = \kappa_u = 1$, $\kappa_c = 30$ is displayed. Middle: same as above, but for $M_{\ell\ell}$ variable. Bottom: normalized $\Delta\phi^{(\ell\ell,\not{E}_T)}$ and $\Delta R^{\ell_2\gamma}$ distributions for signal and SM backgrounds.

[3]Considering only OF events results in a $\sim\sqrt{2}$ reduction in our signal sensitivity. Yet, an experimental analysis splitting the events into OF and SF categories would recover part of this sensitivity. We also note that the SF signal events contain a minor contribution from $h \to ZZ^* \to \nu\bar{\nu}\ell^+\ell^-$.

95% confidence level (C.L.), using a simple $S/\sqrt{B} \simeq 2$ estimate (with S and B being the number of signal and background events) and assuming Higgs boson SM branching fractions.

Given the variety of relevant event kinematic variables and the significant correlations among several of them, it is possible to enhance the signal sensitivity with respect to the above "squared" cut-and-count analysis by accessing the full kinematic information of the events. To this end, we adopt here a multivariate approach and use the following set of kinematic variables (which contains all the relevant kinematic information of each event):

$$M_T, M_{\ell\ell}, M_{\ell\ell\gamma}, p_T^{\ell_1}, p_T^{\ell_2}, p_T^{\gamma}, \not{E}_T,$$
$$\Delta\phi^{\ell\ell}, \Delta\phi^{\ell_1\gamma}, \Delta\phi^{\ell_2\gamma}, \Delta\phi^{(\ell\ell,\not{E}_T)}, \eta^{\ell_1}, \eta^{\ell_2}, \eta^{\gamma} \qquad (3)$$

to train a neural network (NN) to discriminate the $h\gamma$ signal from the various SM backgrounds. The NN architecture uses two hidden layers of 128 and 64 nodes, with rectified linear unit (ReLU) activation for the hidden layers and a sigmoid function for the output layer. The NN is optimized, using as its loss function the binary cross-entropy, using the Adam optimizer [55] (other generalized loss functions such as the one proposed in Ref. [56] do not give an appreciable improvement). Since the experimental dataset is unbalanced—that is, the SM background overwhelms the signal—it is useful to train the NN using more SM background than signal events, so that the NN learns optimally to identify (and reject) the former. Specifically, we use 1.5×10^4 events for the $\ell^+\nu\ell^-\bar{\nu}\gamma$ background, 10^4 events for the $t\bar{t}\gamma$ background, and 5000 events for the $Z\gamma$ ($Z \to \tau^+\tau^-$) background (a total of 3×10^4 SM background events) in the NN training, together with 1.5×10^4 events of the $h\gamma$ signal. The validation set contains the same number of events from each class.

The signal discrimination power achieved by our multivariate analysis is very high, with areas under the "receiver operating characteristic" (ROC) curve of 0.941 and 0.938, respectively, for charm-quark and up-quark Yukawa sensitivity studies. The multivariate NN score variable $\theta_{\rm NN}$ [which may be regarded as a highly nonlinear function of the kinematic variables in Eq. (3)] for the signal and dominant SM backgrounds in the charm-quark Yukawa study is shown in Fig. 3. In this case, a cut in the NN score variable $\theta_{\rm NN} > 0.78$ yields a signal efficiency $\sim$0.57 together with SM background efficiencies 0.057, 0.034, and 0.003, respectively, for $\ell^+\nu\ell^-\bar{\nu}\gamma$, $t\bar{t}\gamma$, and $Z(\to\tau^+\tau^-)\gamma$. For the up-quark Yukawa study, the optimal cut is also found to be $\theta_{\rm NN} > 0.78$, yielding a signal efficiency $\sim$0.56 and respective SM background efficiencies of 0.056, 0.031, and 0.003.

In addition to the dominant SM backgrounds, we also consider the VBF and AP $h + \gamma$ production processes as potential, yet minor backgrounds for our charm and up-quark Yukawa sensitivity analysis, as discussed in Sec. II. The extra high-p_T activity vetoes imposed in our initial event selection suppress these processes down to a $h(\to\ell^+\nu\ell^-\bar{\nu})\gamma$ cross section (assuming SM branching fractions for the Higgs boson) of 32.6 ab for VBF, 2.24 ab for $h\gamma W$ (with $W \to jj$ or $W \to \ell\nu$), and 1.84 ab for $h\gamma Z$ (with $Z \to jj$ or $Z \to \nu\bar{\nu}$), with other backgrounds like $h\gamma j$ and $tth\gamma$ negligible after the event selection. Due to such small cross sections, these backgrounds are not included in the NN training. The NN selection efficiencies for them are the following: in the charm-quark Yukawa study, the cut $\theta_{\rm NN} > 0.78$ yields the efficiencies 0.42, 0.25, and 0.27 for the VBF, $h\gamma W$, and $h\gamma Z$ backgrounds, respectively; for the up-quark Yukawa case, the cut $\theta_{\rm NN} > 0.78$ yields the corresponding efficiencies 0.42, 0.26, and 0.28. Altogether, these backgrounds do not appreciably reduce the sensitivity to κ_c and κ_u from our multivariate analysis, which is driven by the NN ability to reject the main irreducible SM background, $pp \to \ell^+\nu\ell^-\bar{\nu}\gamma$.

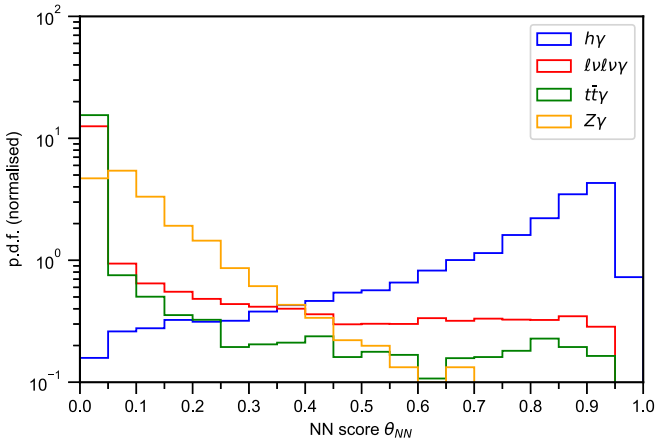

FIG. 3. Multivariate NN score variable $\theta_{\rm NN}$ for the $h\gamma$ signal (blue) and dominant SM backgrounds $\ell^+\nu\ell^-\bar{\nu}\gamma$ (red), $t\bar{t}\gamma$ (green), and $Z(\to\tau^+\tau^-)\gamma$ (yellow) in the charm-quark Yukawa sensitivity study.

IV. CONSTRAINTS ON κ_c AND κ_u

For SM branching fractions of the Higgs boson, the sensitivity to κ_c and κ_u at the HL-LHC from the NN analysis of the previous section is $|\kappa_c| < 11.8$ and $|\kappa_u| < 1930$ at a 95% C.L. (improving on the cut-and-count analysis from Sec. III, as expected). This assumes that the statistical uncertainty of the SM background will largely dominate over its systematic uncertainty at the HL-LHC, which is justified in the present scenario, particularly since the main backgrounds are electroweak processes. The above projected bounds also assume that only one Yukawa coupling of the Higgs boson departs from its SM value.

Enhancing y_c or y_u by an amount that makes them comparable to the SM bottom-quark Yukawa coupling

would modify significantly the total width of the Higgs boson and therefore its branching fractions. Nevertheless, it has long been realized that light quark Yukawa couplings remain essentially unconstrained by global fits to Higgs production and decay rates at the LHC [57–59] (see also Ref. [14]), unless further assumptions are made. The effect of an enhanced Higgs Yukawa coupling y_q to a light quark $q = u$, d, c, s on the Higgs branching fractions may be compensated by a related increase of the Higgs couplings to gauge bosons and third-generation fermions, leading to a "flat direction" in the fit along which the Higgs signal strengths remain unchanged. From the present good agreement between SM predictions and LHC Higgs measurements [22,60,61], this flat direction may be approximately described by a single generic κ_h enhancement factor for all Higgs couplings other than the light quark Yukawa y_q of interest [14]:

$$\kappa_h^2 \simeq \frac{1 - Br_{q\bar{q}}^{\mathrm{SM}}}{2} + \frac{\sqrt{(1 - Br_{q\bar{q}}^{\mathrm{SM}})^2 + 4Br_{q\bar{q}}^{\mathrm{SM}}\kappa_q^2}}{2}, \quad (4)$$

with $Br_{q\bar{q}}^{\mathrm{SM}}$ being the branching fraction for $h \to q\bar{q}$ in the SM. While the combination of Higgs signal strengths with other measurements—e.g., with electroweak precision observables or an indirect measurement of the Higgs total width (model-dependent, see Ref. [62])—can help in lifting the flat direction [Eq. (4)], this discussion highlights the importance of complementary probes of Higgs couplings to light quarks.

Considering κ_c and κ_u along the flat direction defined by Eq. (4) weakens our analysis's sensitivity with respect to the assumption of SM branching fractions, since $\kappa_q > \kappa_h$ for $q = c$, u, and the effect of this becomes particularly important once $y_q/y_b^{\mathrm{SM}} \gtrsim 1$. The projected 95% C.L. sensitivities to κ_c and κ_u along the flat direction are $|\kappa_c| < 26.3$ and $|\kappa_u| < 2300$.

The projected bounds on κ_c which we obtain are complementary to other existing probes in the literature. Yet, they may not be competitive with the most sensitive proposed direct probes of the charm Yukawa coupling [7,9], which yield a current 95% C.L. experimental limit on κ_c (assuming SM Higgs branching fractions) of $\kappa_c \lesssim 13$ [22]. In contrast, the achievable $h\gamma$ sensitivity to κ_u does lie in the same ballpark of other currently proposed probes.

V. CONCLUSIONS

In this paper, we have studied $h\gamma$ production at the HL-LHC. While interesting in its own right, as this process is yet to be observed at the LHC, we demonstrate its role as a sensitive probe of the Higgs boson couplings to the light quarks of the first two generations of matter, still largely unconstrained by present measurements. The associated production with a photon enhances the contribution of the up-type quarks with respect to their down-type counterparts, yielding a way to disentangle Yukawa coupling enhancements from both quark types. This makes $h + \gamma$ highly complementary to other existing light quark Yukawa probes. Concentrating on the $h \to \ell^+\nu\ell^-\bar{\nu}$ decay channel of the Higgs boson, we have performed a multivariate neural network analysis to fully exploit the rich kinematics of this final state, and derived HL-LHC projected sensitivities to the Higgs Yukawa couplings to charm and up quarks. Particularly in the latter case, $h + \gamma$ may help us to gain further insight on Higgs flavor at the LHC.

ACKNOWLEDGMENTS

Feynman diagrams were drawn using TikZ-Feynman [63]. J. A. A. S. acknowledges partial financial support by the Spanish "Agencia Estatal de Investigación" (AEI) through Project No. PID2019–110058GB-C21. The work of J. M. C. was supported by the Spanish Ministerio de Ciencia, Innovación y Universidades (MICIU) and the EU Fondo Social Europeo (FSE) through Grant No. PRE2018-083563. The work of J. M. N. was supported by Ramón y Cajal Fellowship Contract No. RYC-2017-22986, and by Grant No. PGC2018-096646-A-I00 from the Spanish Proyectos de I + D de Generación de Conocimiento. J. M. N. also acknowledges support from the European Union's Horizon 2020 research and innovation programme under Marie Sklodowska-Curie Grant Agreement No. 860881 (ITN HIDDeN), as well as from the AEI through Grant IFT Centro de Excelencia Severo Ochoa No. SEV-2016-0597.

[1] G. T. Bodwin, F. Petriello, S. Stoynev, and M. Velasco, Phys. Rev. D **88**, 053003 (2013).
[2] A. L. Kagan, G. Perez, F. Petriello, Y. Soreq, S. Stoynev, and J. Zupan, Phys. Rev. Lett. **114**, 101802 (2015).
[3] F. Goertz, Phys. Rev. Lett. **113**, 261803 (2014).
[4] G. Perez, Y. Soreq, E. Stamou, and K. Tobioka, Phys. Rev. D **92**, 033016 (2015).
[5] G. Perez, Y. Soreq, E. Stamou, and K. Tobioka, Phys. Rev. D **93**, 013001 (2016).
[6] M. Knig and M. Neubert, J. High Energy Phys. 08 (2015) 012.
[7] I. Brivio, F. Goertz, and G. Isidori, Phys. Rev. Lett. **115**, 211801 (2015).
[8] Y. Soreq, H. X. Zhu, and J. Zupan, J. High Energy Phys. 12 (2016) 045.

[9] F. Bishara, U. Haisch, P. F. Monni, and E. Re, Phys. Rev. Lett. **118**, 121801 (2017).
[10] G. Bonner and H. E. Logan, arXiv:1608.04376.
[11] F. Yu, J. High Energy Phys. 02 (2017) 083.
[12] J. Cohen, S. Bar-Shalom, G. Eilam, and A. Soni, Phys. Rev. D **97**, 055014 (2018).
[13] S. Mao, Y. Guo-He, L. Gang, Z. Yu, and G. Jian-You, J. Phys. G **46**, 105008 (2019).
[14] N. M. Coyle, C. E. M. Wagner, and V. Wei, Phys. Rev. D **100**, 073013 (2019).
[15] L. Alasfar, R. Corral Lopez, and R. Grber, J. High Energy Phys. 11 (2019) 088.
[16] G. Aad *et al.* (ATLAS Collaboration), Phys. Rev. Lett. **114**, 121801 (2015).
[17] M. Aaboud *et al.* (ATLAS Collaboration), Phys. Rev. Lett. **117**, 111802 (2016).
[18] X. C. Vidal *et al.* (LHCb Collaboration), Reports No. LHCb-CONF-2016-006, No. CERN-LHCb-CONF-2016-006, 2016.
[19] M. Aaboud *et al.* (ATLAS Collaboration), J. High Energy Phys. 07 (2018) 127.
[20] M. Aaboud *et al.* (ATLAS Collaboration), Phys. Rev. Lett. **120**, 211802 (2018).
[21] A. M. Sirunyan *et al.* (CMS Collaboration), J. High Energy Phys. 11 (2020) 039.
[22] G. Aad *et al.* (ATLAS Collaboration), Eur. Phys. J. C **80**, 942 (2020).
[23] R. A. Porto and A. Zee, Phys. Lett. B **666**, 491 (2008).
[24] G. F. Giudice and O. Lebedev, Phys. Lett. B **665**, 79 (2008).
[25] M. Bauer, M. Carena, and K. Gemmler, J. High Energy Phys. 11 (2015) 016.
[26] M. Bauer, M. Carena, and K. Gemmler, Phys. Rev. D **94**, 115030 (2016).
[27] W. Altmannshofer, J. Eby, S. Gori, M. Lotito, M. Martone, and D. Tuckler, Phys. Rev. D **94**, 115032 (2016).
[28] W. Altmannshofer, S. Gori, D. J. Robinson, and D. Tuckler, J. High Energy Phys. 03 (2018) 129.
[29] D. Egana-Ugrinovic, S. Homiller, and P. R. Meade, Phys. Rev. D **100**, 115041 (2019).
[30] F. Bishara, J. Brod, P. Uttayarat, and J. Zupan, J. High Energy Phys. 01 (2016) 010.
[31] A. Abbasabadi, D. Bowser-Chao, D. A. Dicus, and W. W. Repko, Phys. Rev. D **58**, 057301 (1998).
[32] E. Gabrielli, B. Mele, and J. Rathsman, Phys. Rev. D **77**, 015007 (2008).
[33] P. Agrawal and A. Shivaji, Phys. Lett. B **741**, 111 (2015).
[34] E. Gabrielli, B. Mele, F. Piccinini, and R. Pittau, J. High Energy Phys. 07 (2016) 003.
[35] K. Arnold, T. Figy, B. Jager, and D. Zeppenfeld, J. High Energy Phys. 08 (2010) 088.
[36] H. Khanpour, S. Khatibi, and M. Mohammadi Najafabadi, Phys. Lett. B **773**, 462 (2017).
[37] B. A. Dobrescu, P. J. Fox, and J. Kearney, Eur. Phys. J. C **77**, 704 (2017).
[38] W. H. Furry, Phys. Rev. **51**, 125 (1937).
[39] M. Peskin and D. Schroeder, *An Introduction to Quantum Field Theory* (CRC Press, 1995), p. 318.
[40] S. P. Martin and D. G. Robertson, Phys. Rev. D **100**, 073004 (2019).
[41] J. Alwall, R. Frederix, S. Frixione, V. Hirschi, F. Maltoni, O. Mattelaer, H.-S. Shao, T. Stelzer, P. Torrielli, and M. Zaro, J. High Energy Phys. 07 (**2014**) 79.
[42] V. Bertone, S. Carrazza, N. P. Hartland, and J. Rojo (NNPDF Collaboration), SciPost Phys. **5**, 008 (2018).
[43] Trigger Menu in 2017, Technical Report No. ATL-DAQ-PUB-2018-002, CERN, Geneva, 2018.
[44] M. Ishino, EPJ Web Conf. **164**, 07003 (2017).
[45] M. Aaboud *et al.* (ATLAS Collaboration), Eur. Phys. J. C **77**, 361 (2017).
[46] A. M. Sirunyan *et al.* (CMS Collaboration), Eur. Phys. J. C **78**, 965 (2018).
[47] G. Aad *et al.* (ATLAS Collaboration), J. High Energy Phys. 03 (2020) 054.
[48] T. Sjstrand, S. Ask, J. R. Christiansen, R. Corke, N. Desai, P. Ilten, S. Mrenna, S. Prestel, C. O. Rasmussen, and P. Z. Skands, Comput. Phys. Commun. **191**, 159 (2015).
[49] J. de Favereau, C. Delaere, P. Demin, A. Giammanco, V. Lematre, A. Mertens, and M. Selvaggi (DELPHES 3 Collaboration), J. High Energy Phys. 02 (2014) 057.
[50] M. Cacciari, G. P. Salam, and G. Soyez, J. High Energy Phys. 04 (2008) 063.
[51] M. Cacciari, G. P. Salam, and G. Soyez, Eur. Phys. J. C **72**, 1896 (2012).
[52] D. Bertolini, P. Harris, M. Low, and N. Tran, J. High Energy Phys. 10 (2014) 059.
[53] M. Cacciari, G. P. Salam, and G. Soyez, Eur. Phys. J. C **75**, 59 (2015).
[54] P. Berta, M. Spousta, D. W. Miller, and R. Leitner, J. High Energy Phys. 06 (2014) 092.
[55] D. P. Kingma and J. Ba, Adam: A method for stochastic optimization, arXiv:1412.6980.
[56] C. W. Murphy, SciPost Phys. **7**, 076 (2019).
[57] D. Zeppenfeld, R. Kinnunen, A. Nikitenko, and E. Richter-Was, Phys. Rev. D **62**, 013009 (2000).
[58] M. Duhrssen, S. Heinemeyer, H. Logan, D. Rainwater, G. Weiglein, and D. Zeppenfeld, Phys. Rev. D **70**, 113009 (2004).
[59] G. Belanger, B. Dumont, U. Ellwanger, J. Gunion, and S. Kraml, Phys. Rev. D **88**, 075008 (2013).
[60] CMS Collaboration, Report No. CMS-PAS-HIG-19-005, 2020.
[61] G. Aad *et al.* (ATLAS Collaboration), Phys. Rev. D **101**, 012002 (2020).
[62] C. Englert and M. Spannowsky, Phys. Rev. D **90**, 053003 (2014).
[63] J. Ellis, Comput. Phys. Commun. **210**, 103 (2017).